

Bulk and Surface Electronic Structure of the Layered Sub-Nitrides Ca_2N and Sr_2N

C. M. Fang,^{*,†} G. A. de Wijs,[‡] R. A. de Groot,^{‡,§} H. T. Hintzen,[†] and G. de With[†]

Laboratory of Solid State and Materials Chemistry, Eindhoven University of Technology, Postbox 513, 5600 MB Eindhoven, The Netherlands, Electronic Structure of Materials, Research Institute for Materials, Toernooiveld 1, 6525 ED Nijmegen, The Netherlands, and Laboratory of Chemical Physics, MSC, Nijenborg 4, 9747 AG Groningen, The Netherlands

Received February 8, 2000. Revised Manuscript Received March 30, 2000

The binary sub-nitrides M_2N ($\text{M} = \text{Ca}$ and Sr) have the anti- CdCl_2 layered structure. First-principles calculations show that these sub-nitrides are best described as ionic compounds with one electron in the “van der Waals gap” between the calcium (strontium) layers. The nitrogen 2p states show rather localized character with a bandwidth of about 2 eV. The compounds have a quasi-two-dimensional electronic structure with a cylindrical Fermi surface perpendicular to the layer direction. Calculations also show that the surface M_2N slab has density of N 2s, 2p states shifted toward to a lower energy (about 1 eV) with respect to the bulk. These layered compounds may have an application as cathode material for polymer LED devices.

I. Introduction

This paper addresses three problems concerning the electronic structure of Ca_2N and Sr_2N . In the first place, we discuss the intrinsic electronic transport properties and the bulk electronic structure of Ca_2N and Sr_2N . Second, we investigate surface effects of the layered crystals, to understand the photoelectron spectra of Ca_2N and Sr_2N . Finally, we study the effects of quantum confinement of electrons in a thin film of Ca_2N and Sr_2N . The possible application of such layered sub-nitrides as a cathode material for the polymer light emission diodes (LED) is also discussed.

Alkaline earth sub-nitrides Ca_2N and Sr_2N have the layered anti- CdCl_2 structure.^{1,2} Sr_2N was first synthesized and determined to have a layered structure by Gaudé et al.¹ However, Brice et al. claimed that Sr_2N was actually $\text{Sr}_3\text{N}_{2-x}\text{H}_x$ ($0.4 \leq x \leq 1$) or Sr_2NH_2 on the basis of chemical analysis.³ Hulliger also questioned the existence of the alkaline earth sub-nitrides (M_2N), because they had been reported to be nonmetallic.⁴ Brese and O’Keeffe synthesized Sr_2N by nitridation of Sr metal and determined the crystal structure by time-of-flight neutron diffraction.⁵ They confirmed the layered structure and found no trace of H in the structure. The structure of Ca_2N was determined from single-crystal X-ray data by Keve and Skapski.^{2,6}

The crystals of Ca_2N and Sr_2N have a lustrous appearance. However, experimental data on the intrinsic electrical conductivity are controversial. Keve and Skapski⁶ found that the conductivity of Ca_2N is in the semiconductor range (about 20 S m^{-1} at room temperature) and increases with increasing temperature as for a semiconductor. Sr_2N was first reported to have a conductivity of $500 \text{ (S m}^{-1})$.⁴ Later measurements showed that Sr_2N has a conductivity of 6000 S m^{-1} at room temperature and that the conductivity decreases with increasing temperature,⁵ as for a metal. Recently Steinbrenner et al.⁷ reported the study of photoelectron spectra of some alkaline earth metal sub-nitrides, including Ca_2N and Sr_2N . They also presented the density of N 2p states for the sub-nitrides obtained from LMTO-ASA calculations. The photoelectron spectra showed two broad peaks at about 2.4 and 3.4 eV for Ca_2N and at about 2.0 and 2.8 eV below the Fermi level for Sr_2N . The UPS spectra of Ca_2N and Sr_2N were found to be more structured than the calculated density of states (DOS) curves.

II. Ab Initio Band Structure Calculations

A. Crystal Structure. Sr_2N and Ca_2N crystallize in the layered anti- CdCl_2 structure, with space group $R\bar{3}m$. The lattice parameters are listed in Table 1. The nitrogen lies at $\bar{3}$ and is in trigonal-antiprismatic (approximately octahedral) coordination by Sr (Ca) with an identical N–Sr (N–Ca) distance of 2.6118 Å (2.433 Å). The Sr–Sr distances in the layer are 3.8566 Å ($6\times$) and 3.523 Å ($3\times$). The interlayer Sr–Sr distance is 4.726 Å, much larger than in pure Sr metal (4.303 Å).⁸⁸ In

[†] Eindhoven University of Technology.

[‡] Research Institute for Materials.

[§] Laboratory of Chemical Physics.

(1) Gaudé J.; L’Haridon, P.; Laurent, Y.; Lang, J. *Bull. Soc. Fr. Mineral. Cristallogr.* **1972**, *95*, 56.

(2) Keve, E. T.; Skapski, A. C. *Chem. Commun.* **1966**, 829.

(3) Brice, J.-F.; Motte, J.-P.; Aubry, J. *Rev. Chim. Mineral.* **1975**, *12*, 105.

(4) Hulliger, F. In *Structural Chemistry of Layer-type Phases*; Levy, F., Ed.; Reidel: Dordrecht, Holland, 1976.

(5) Brese, N. E.; O’Keeffe, M. *J. Solid State Chem.* **1990**, *87*, 134.

(6) Keve, E. T.; Skapski, A. C. *Inorg. Chem.* **1968**, *7*, 1757.

(7) Steinbrenner, U.; Adler, P.; Holle, W.; Simon, A. *J. Phys. Chem. Solids* **1998**, *59*, 1527.

(8) Wyckoff, R. W. G. *Crystal Structures*; Wiley: New York, 1965; Vol. 3.

Table 1. Space Group, Unit-Cell Dimensions, the Ratios d/a per Sandwich, the Number of Formula Units per Cell (Z), Coordinates of Metal (u_M), and the M–M and M–X Distances of the Binary Nitrides M_2N ; Metal–Metal Distances in Pure Metals^a Are Included in Parentheses for Comparison

	space group	a (Å)	c (Å)	u_M	Z	d/a	d_{M-M} (Å)	d_{M-X} (Å)
Ca_2N	$R\bar{3}m^6$	3.638	18.78	0.268	3	1.721	2.433	4.347 (3.877, γ -Ca) (3.947, α -Ca)
Sr_2N	$R\bar{3}m^5$	3.8566	20.6958	0.2674	3	1.789	2.612	4.726 (4.303, Sr)

Ca_2N the intralayer Ca–Ca distances are 3.638 Å ($6\times$) and 3.230 Å ($3\times$). The interlayer Ca–Ca distances are also large (Table 1). In this paper we will refer to a “slab” as an entity comprising a M–N–M ($M = Ca, Sr$) trilayer and the phrase “layer” for the one-atom layer case.

B. Details of the Calculations. The electronic structure of the bulk nitrides was calculated with both the pseudo-potential (PP)^{9–11} and the localized spherical wave (LSW) method.¹² Contrary to the LSW method, the PP calculations do not employ the atomic-sphere approximation (ASA), and therefore they are a good benchmark for the LSW calculations. Having established the validity of the ASA with the bulk calculations, the ASA-LSW was used for computationally more demanding studies on the slab and film.

For the PP calculations we used the ab initio total energy and molecular dynamics program VASP (Vienna *Ab-initio* Simulation Program), developed by the Institut für Theoretische Physik of the Technische Universität Wien (who also supplied the pseudo-potentials).⁹ Vanderbilt-type ultrasoft pseudo-potentials¹⁰ were used, with a frozen [Ne]3s², [Ar]3d¹⁰4s², and 1s² core for Ca, Sr, and N, respectively. Nonlinear core corrections were applied for Ca and Sr.¹¹ The Kohn–Sham orbitals were expanded in plane waves with a kinetic energy cutoff of 32 Ry. A $10 \times 10 \times 10$ Monkhorst–Pack grid was used to sample the Brillouin zone (BZ), resulting in 110 k -points in the irreducible BZ part.

To describe the density of states in terms of atomic wave functions, calculations were performed with the localized spherical wave (LSW) method,^{12,13} which is very efficient for large systems. In this method the potential is represented by spherically averaged potentials in overlapping space-filling spheres centered at the atomic nuclei (ASA). It is known that within ASA the electronic structure could be dependent on the specific choice of sphere radii. Therefore, the sphere radii of the atoms were taken according to the radii¹⁴ of N^{3-} , Ca^{2+} , and Sr^{+} .

The self-consistent calculations using the LSW method were carried out including all core electrons. Iterations were performed with k -points distributed uniformly in an irreducible part of the first Brillouin zone (BZ), corresponding to a volume of the BZ per k -point of the order of 1×10^{-6} Å⁻³. In the construction of the LSW basis,¹² the spherical waves were augmented by solutions of the scalar-relativistic radial equations as indi-

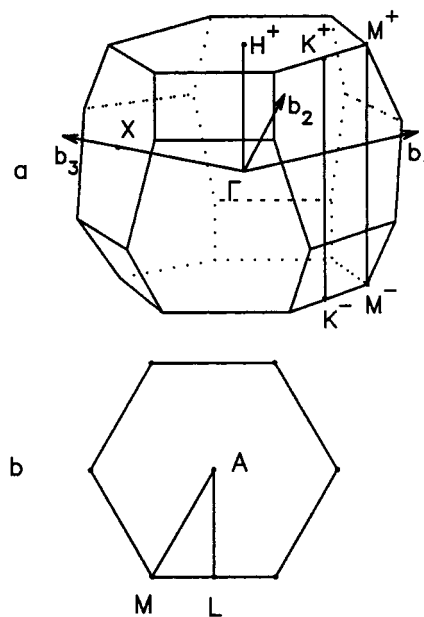


Figure 1. Brillouin zone and high symmetry points for the binary nitrides (a) and for the single M_2N slab in the layer directions (b).

Table 2. Input Parameters for the LSW Calculations (Coordinates of Atoms and Empty Spheres (Va), Wigner–Seitz Radii (R_{WS}) and Calculated Electronic Configurations; Lattice Parameters and Space Group Are Listed in Table 1

	WP coordinates	R_{WS} (Å)	electronic configuration
Ca_2N			
N 3a	(0, 0, 0)	1.7266	[He] 2s ^{1.96} 2p ^{5.22} 3d ^{0.02}
Ca 6c	(0, 0, 0.2680)	1.0884	[Ar] 4s ^{0.04} 4p ^{0.05} 3d ^{0.15} 4f ^{0.01}
Va 3b	(0, 0, 0.5)	1.9313	1s ^{0.86} 2p ^{0.34} 3d ^{0.10}
Sr_2N			
N 3a	(0, 0, 0)	1.7266	[He] 2s ^{1.96} 2p ^{5.17} 3d ^{0.01}
Sr 6c	(0, 0, 0.26737)	1.2431	[Kr] 4s ^{0.05} 4p ^{0.05} 3d ^{0.16} 4f ^{0.01}
Va 3b	(0, 0, 0.5)	2.3035	1s ^{0.88} 2p ^{0.32} 3d ^{0.10}

cated in Table 2. Because the crystals of the layered compounds are not very densely packed, it is necessary to include empty spheres (Va) in the calculations.

Both the PP method and the LSW method are based on density functional theory (DFT), with the exchange correction energy treated within the local density approximation (LDA). Scalar relativistic effects were included in the calculations. Experimental equilibrium lattice parameters and atomic positions were used (Table 1).

C. Electronic Structure of Bulk M_2N . Figure 1a shows the Brillouin zone (BZ)¹⁵ of the nitrides with the space group $R\bar{3}m$. The dispersion curves of the energy bands along the high-symmetry lines by the PP method are shown in Figures 2 and 3 for bulk Ca_2N and Sr_2N ,

(9) Kresse, G.; Hafner, J. *Phys. Rev.* 1993, *B47*, 558; **1994**, *49*, 14251. Kresse, G.; Furthmüller, J. *Comput. Mater. Sci.* **1996**, *6*, 15. Kresse, G.; Furthmüller, J. *Phys. Rev.* **1996**, *B54*, 11169.

(10) Vanderbilt, D. *Phys. Rev.* 1990, *B41*, 7892. Kresse, G.; Hafner, J. *J. Phys.: Condens. Matter* **1994**, *6*, 8245.

(11) Louie, S. G.; Froyen, S.; Cohen, M. L. *Phys. Rev.* **1982**, *B26*, 1738.

(12) van Leuken, H.; Lodder, A.; Czyzyk, M. T.; Springelkamp, F.; de Groot, R. A. *Phys. Rev.* **1990**, *B41*, 5613.

(13) Anderson, O. K. *Phys. Rev.* **1975**, *B8*, 3060.

(14) *CRC Handbook of Chemistry and Physics*, 61st ed.; CRC Press: Boca Raton, FL, 1980.

(15) Miller, S. C.; Love, W. F. *Table of Irreducible Representations of Space Groups and Representations of Magnetic Space Groups*; Prentice Press: Boulder, CO, 1967.

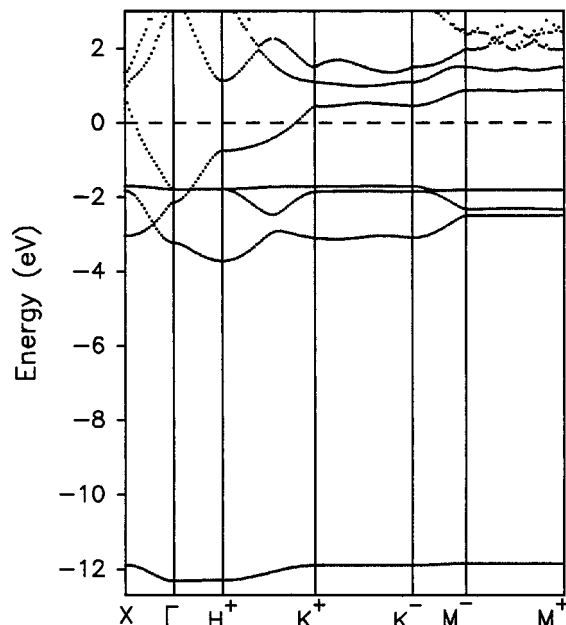


Figure 2. Dispersion curves of the energy bands for bulk Ca_2N by the PP method.

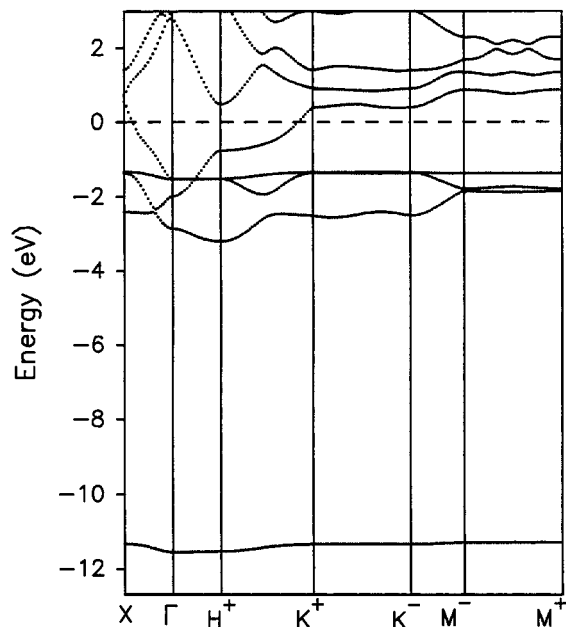


Figure 3. Dispersion curves of the energy bands for bulk Sr_2N by the PP method.

Table 3. Comparison of Calculated Electronic Structure of Ca_2N and Sr_2N (All Values in eV)

	Ca_2N			Sr_2N		
	PP	LMTO ⁷	LSW	PP	LMTO ⁷	LSW
bottom of VB	-3.77	-3.86	-3.78	-3.25	-3.16	-3.21
width of N 2p	1.95	1.30	2.0	1.60	1.1	1.8
top of the VB	0.9	1.9	1.3	1.0	1.85	1.1
width of N 2s			0.41			0.38
position of N 2s	-12.20	-13.0	-12.13	-11.47	-12.4	-11.49

respectively. The input parameters for calculations for the bulk sub-nitrides using the LSW method are listed in Table 2.

Table 3 compares general features of the electronic structure of the alkaline earth sub-nitrides obtained by the different methods. In general, the three sets of calculated results are similar. However, the electronic

structure calculated by the LSW method is clearly in better agreement with the PP results than with the LMTO calculations by Steinbrenner et al.⁷ For example, the shape and position of the N 2p band coincide much better. On the other hand, minor differences between the LSW and PP calculations exist: in the band structure along the K^+ to K^- direction, in the LSW calculations, the N 2p bands are evenly split, while in the PP calculations the two highest levels are almost degenerate. The differences between the LSW and LMTO calculations mainly originate from the different choice of the Wigner–Seitz radii for the atoms and the empty spheres and the choice of the orbitals for the metal atoms. In the LMTO study,⁷ small Wigner–Seitz radii (1.267–1.437 Å) for nitrogen atoms and large radii for the metals (1.668 Å for Ca and 1.833 Å for Sr) were employed. The Ca 4p (Sr 5p) orbitals were neglected.

Table 2 also lists the calculated electronic configurations for the sub-nitrides from the LSW method. We remark that the number of electrons on an atom (ion) cannot be uniquely defined. We use the number of electrons in the Wigner–Seitz spheres. The electronic configurations are dependent on the size of Wigner–Seitz spheres employed, and the absolute value of these numbers should be interpreted with care. However, the difference between charges of same chemical species with the same Wigner–Seitz radius is meaningful.

Here we discuss the details of the electronic structure of the sub-nitrides from the LSW approach, combined with the PP results. The calculated electronic configurations show that the compounds can be described as ionic, which is shown from the full occupation of N 2p states (Figures 2–5). The metal atoms have a valence of about 2+. There are about 1.3 electrons (Va) in the “van der Waals gap”.

Both binary sub-nitrides have similar electronic structures, as shown in Figures 2–5, due to the fact that both compounds have the same type of structure, and both metals have similar electronegativities. There are some differences in details. The band structures are composed of two main bands separated by an energy gap. The N 2s states of both compounds form a narrow band of about 0.4 eV. The N 2s band of Ca_2N is lower in energy (from -12.2 to -11.8 eV) than that of Sr_2N (from -11.5 to -11.2 eV). The dispersion of the N 2s band across the “van der Waals gap” between the Ca (Sr) layers (along the Γ – H^+ direction) is very small, as compared to that in the intralayer direction (e.g., along H^+ – K^+).

The valence bands (the bands near the Fermi level) are mainly composed of N 2p states mixed with a nonnegligible amount of Ca 4s, 4p (Sr 5s, 5p) character. But the bottom of the valence bands for both sub-nitrides are at H (H^+) in the BZ, with N 2p_z states hybridized with a small amount of Ca 4s (Sr 5s) states. The Ca 4s (Sr 5s) states are at the bottom of the valence band, while the Ca 4p (Sr 5p) states are positioned somewhat higher in energy. The highest density of the N 2p states is about 1.3 and 1.0 eV below the Fermi level for Ca_2N and Sr_2N , respectively. The dispersion of the N 2p band is in general not large, due to the nonbonding character. The strongest dispersion curves of two of the bands in the \mathbf{k}_z direction (Γ – H^+) are mainly composed of N 2p_z (bottom at H^+ , bonding) and Ca 4p_z

(Sr $5p_z$) (top at H^+ below E_F , antibonding) character. The overlap between the N $2p_z$ and Ca $4p_z$ (Sr $5p_z$) in the slab and Ca $4p_z$ (Sr $5p_z$) across the "van der Waals gap" is quite large, leading to a total bandwidth of about 3.0 and 2.7 eV for Ca_2N and Sr_2N , respectively. It indicates that the interlayer interactions are rather strong. Nevertheless, there is no net bonding across the "van der Waals gap" because both bonding and antibonding states are occupied. (It is worthwhile to note that interactions should not be confused with bonding, which is the sum of all interactions.) The differences between Ca_2N and Sr_2N are mainly due to the size effect, i.e., the difference in ionic radii for Ca and Sr.

There is no band crossing the Fermi level in the high-symmetry directions associated with the "van der Waals gap" ($\Gamma-H^+$, K^+-K^- , and M^+-M^-) for both Sr_2N and Ca_2N . Bands cross the Fermi level in the layer directions ($\Gamma-X$ and H^+-K^+). The Fermi surface shows a two-dimensional character for both Sr_2N and Ca_2N : a cylinder along the interlayer direction. The valence band near the Fermi level is dominated by states in interlayer space. The parabolic shape of the bands along H^+-M^+ and H^+-K^+ as well as the flatness of the density of states around the Fermi level (E_F) indicates that the behavior of the electrons around E_F is that of a two-dimensional free electron gas confined in between the slabs.

D. Electronic Structure of a Single M_2N Slab.

The electronic structure was calculated, using only the LSW method, for a single slab of M_2N ($M = Ca$ and Sr). The local point symmetry of the system is kept for nitrogen (at $\bar{3}$), but the space group of the single slab is reduced from $R\bar{3}m$ to $P\bar{3}m1$. The Brillouin zone is shown in Figure 1b. The distance between the slabs is taken sufficiently large ($>16.3 \text{ \AA}$), so that interactions between the slabs are negligible.

The calculated electronic configurations show that in the single slab there are about 5.30 electrons in the N $2p$ orbitals, slightly more than that in the bulk (5.22 electrons), and 0.28 electrons in Ca, which is also a little bit more than in the bulk (0.25 electrons). There are 0.55 electrons in the nearest empty spheres, less than half of the corresponding bulk value.

Figures 6 and 7 show the DOS and the dispersion of the energy bands of a single slab of Ca_2N , respectively. They are similar in many respects to that of the bulk. This is in agreement with the fact that the main features of the electronic structure are determined by the strong intralayer interactions. The flatness of the density of states at the Fermi energy (E_F) extends to higher energy as compared with that of the bulk. This, again, reflects the free-electron-like character of the charge carriers. However, we also observe important differences between the single slab and the bulk electronic structure. The N $2s$ band becomes narrower (0.25 eV) than in the bulk (0.4 eV). The band also shifts about 1.0 eV toward lower energies. The N $2p$ band has a width of about 1.35 eV, compared to 2.3 eV in the bulk in the LSW approach. The bottom of the N $2p$ band also shifts about 0.3 eV toward the lower energy. The N $2p$ band is separated from the band crossing the Fermi level.

Figure 8 shows the dispersion of the single Sr_2N slab. The N $2p$ bands are between -2.80 and -1.89 eV,

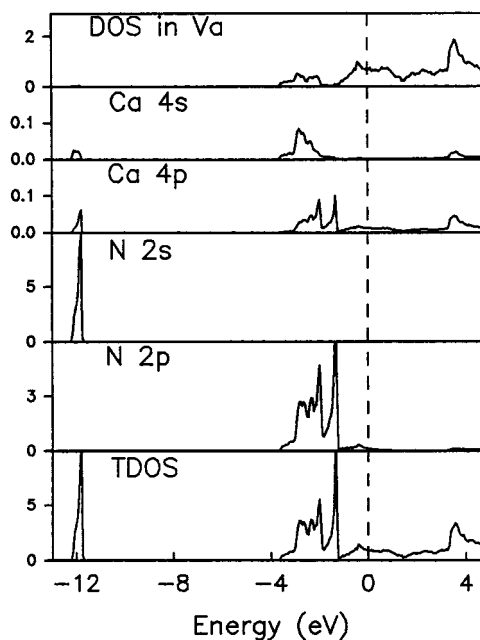


Figure 4. Partial and total density of states for bulk Ca_2N by the LSW method. The Fermi level (E_F) is set at 0 eV, which is the same as in Figures 5, 6, and 9.

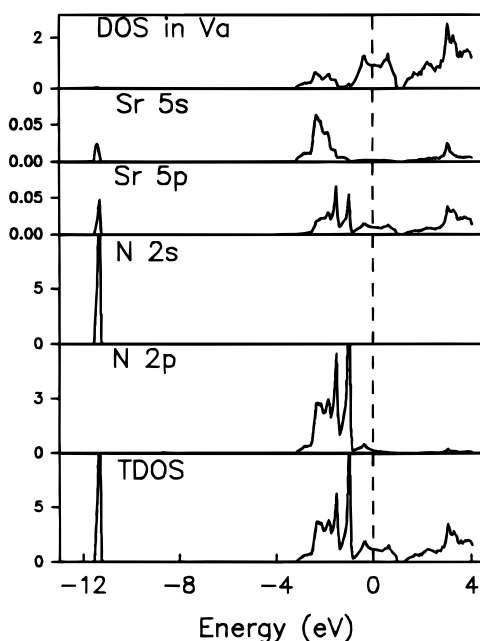


Figure 5. Partial and total density of states for bulk Sr_2N by the LSW method.

separated from the upper valence band, as in the single Ca_2N slab. There are about 0.15 electrons more in the N $2p$ orbitals in the single Sr_2N slab than in the bulk, again, similar to that in the case of Ca_2N . However, the N $2p$ band is broader for the single Sr_2N slab than the single Ca_2N slab.

E. Electronic Structure of a Thin Film of Ca_2N .

Band structure calculations were performed for a thin film of Ca_2N using the LSW method. The thin film is built of 13 Ca_2N slabs with a large distance ($>16.3 \text{ \AA}$) between the films.

The numbers of electrons in the atomic spheres of the same chemical species, deep inside the thin film and at the surface, are similar. Only the N atom of the surface

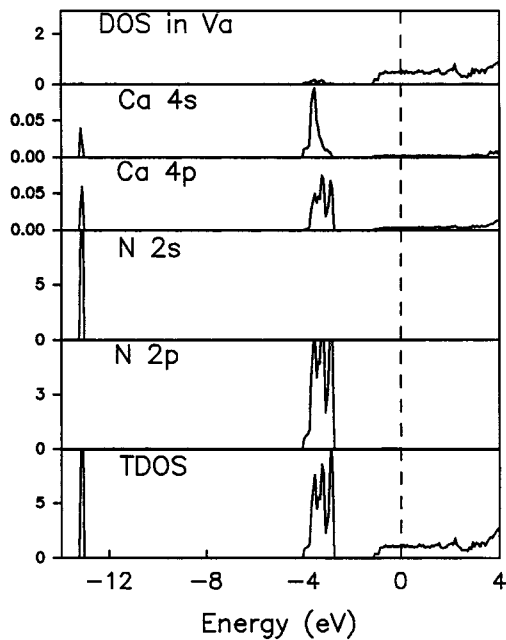


Figure 6. Partial density of states for a single slab of Ca_2N .

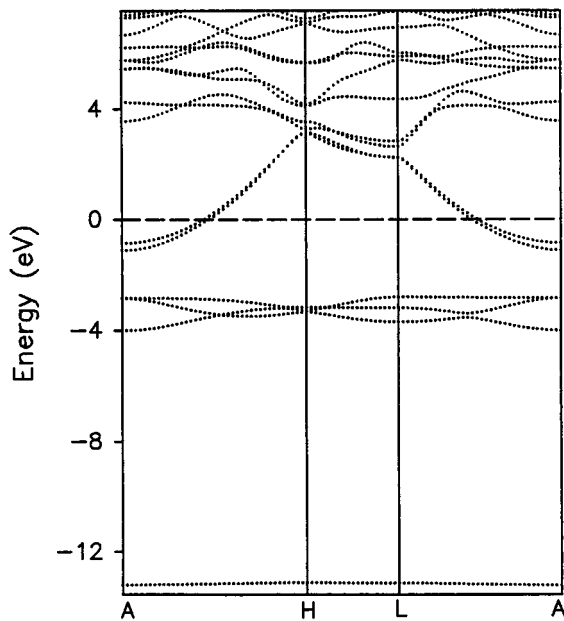


Figure 7. Dispersion curves of the energy bands for a single slab of Ca_2N .

slab has about 0.1 electrons more than in the bulk. Differences are larger in the vacuum region at the surface: There are about 0.50 electrons in the empty sphere outside of the surface, less than half of the inner empty spheres.

Figure 9 shows the partial DOS of the thin film Ca_2N . The outermost slab of the thin film is different significantly from the inner layers (or bulk). The electronic structure of the outermost Ca_2N has the combined characteristics of the single slab and the bulk. The N 2s states range from -12.85 to -12.45 eV, which have the same bandwidth as the inner slabs, but are shifted about 0.8 eV toward the lower energy, as found for the single Ca_2N slab (Figures 6 and 7). The shape of the band of the surface slab is affected, but the bandwidth maintains approximately the same (Figure 9). The N 2p bands become separated from the uppermost part of

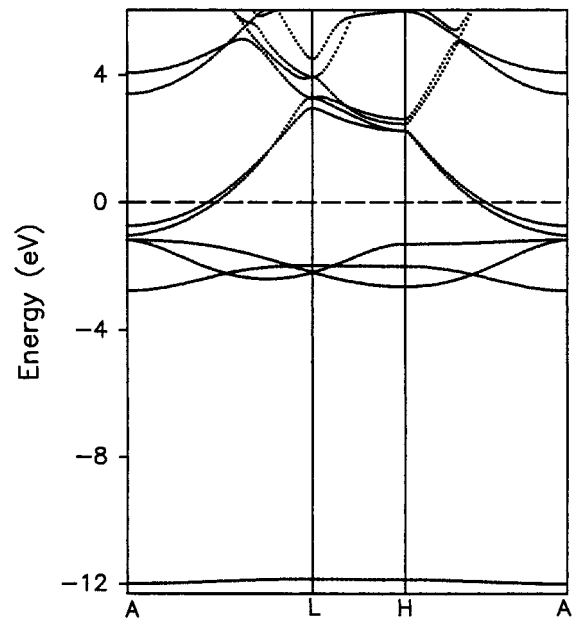


Figure 8. Dispersion curves of the energy bands for a single slab of Sr_2N .

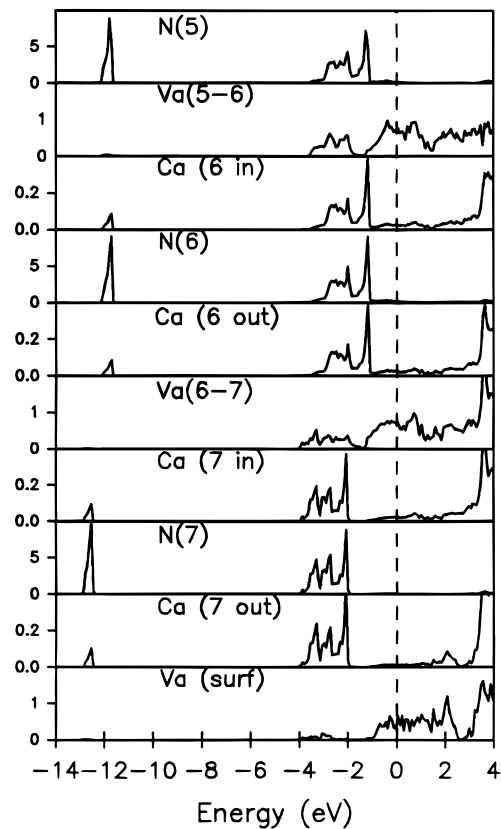


Figure 9. Partial density of states of the outside layers of a thin film of Ca_2N . Numbers are used to indicate a slab from the surface (7) to center (1).

the valence band, like in the single slab case (Figure 6). The free electrons outside the thin film dominate the valence band around the Fermi level.

Figure 10 shows the Madelung energy of the atoms along the interlayer direction obtained from the band structure calculation for a film of 13 slabs Ca_2N . The Madelung energy is the same for all inner N atoms, while it is about 1.85 eV lower for the N in the outermost layer. For Ca atoms it is a little more complicated: The

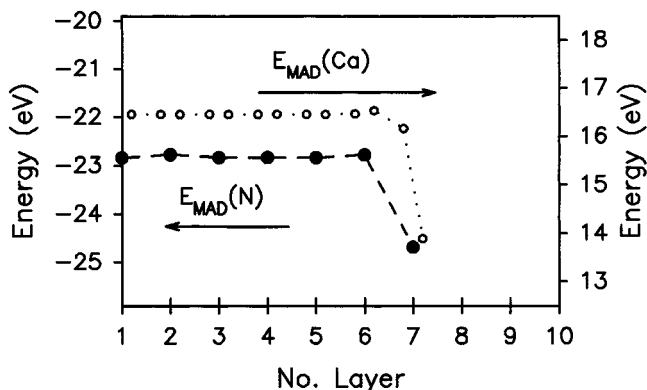


Figure 10. Madelung energy of the atoms along Z direction for half of the thin film of Ca_2N . The number represents a slab from surface (7) to center.

Madelung energy of the Ca in the outermost and the next-outermost layer is about 2.56 and 0.30 eV lower than that in the inner layer. The third layer Ca next to the surface has the Madelung energy about 0.1 eV higher than the inner layers. These differences in Madelung energy have strong influence on the surface electronic structure for the layer sub-nitrides.

III. Discussion

Recently, photoemission spectra of the powdered binary sub-nitrides were reported.⁷ There are two rather broad N 2p peaks at about 2.4 and 3.4 eV below the Fermi level for Ca_2N and about 2.0 and 2.8 eV below the Fermi level for Sr_2N . In their calculated results the DOS peaks (mainly N 2p states) are found to be at higher energies (~ 1 eV).⁷ Also, a discrepancy exists when comparing the photoelectron spectra with the calculated position of the N 2s states (~ 1 eV) and the position of the semicore Ca and Sr level in the PP calculations (~ 2 eV).⁷

We remark that photoemission spectroscopy is a very surface-sensitive technique. The mean free path of the electron escaping from the metallic solids is estimated from Penn's relation¹⁶ to be very short (a few angstroms) for photoelectrons with an energy of about 20 eV. Because the thickness of a single slab Ca_2N is about 6 Å, the photoemission signal originates mainly from the outermost surface layer. Therefore, the information obtained from photoelectron spectra concerns mostly the electronic structure of the outermost layers of the solids.

(16) Penn, D. R. *J. Electron Spectrosc.* **1976**, *9*, 29. Seah, M. P.; Dench, W. A. *Surf. Interface Anal.* **1979**, *1*, 2.

The partial DOS for the surface slab Ca_2N shows a single peak at -3.32 eV and two peaks at -2.75 and -2.10 eV. Those peaks are in good agreement with the photoelectron spectra of Ca_2N , which is composed of two broad peaks at -3.4 and -2.4 eV. The latter peak corresponds to the two broad calculated peaks at -2.75 and -2.10 eV. It must be realized that the comparison between a calculated (ideal) surface and experimental data obtained for "mixed" surfaces at powdered samples complicates the analyses. The surface effect can also explain part of the discrepancy between the experimental and calculated positions of the N 2s and the semicore states.

In the bulk N 2p states are positioned about 1 eV below the Fermi level and have almost no density in the bands crossing the Fermi level. The N^{3-} ions repel the "free" electrons, and the interlayer Ca-Ca (Sr-Sr) distances become much larger than those in the pure metals (Table 1). Also, the N^{3-} ions form blocking layers and confine the electrons in the "van der Waals gap" to form a two-dimensional electron gas. One effect of quantum confinement is that the work functions of these nitrides are expected to be lower than those of the corresponding metals, as in the case of cesium suboxides.^{17,18} Low work function materials, such as Ca, are employed as electron-injecting contacts on polymer LED's. The drawback of the use of calcium is that it is so reactive.¹⁹ The sub-nitrides may be an alternative because of their low work functions and reduced reactivity.^{20,21}

Acknowledgment. Prof. Dr. G. A. Wiegers (RUG) and Drs. Joost Hageman (KUN) are acknowledged for beneficial discussions and critical reading of the manuscript. Dr. Kees Flipse (FOG, TUE) is thanked for discussion about the photoelectron spectra. This work was part of the research program of the Stichting voor Fundamenteel Onderzoek der Materie (FOM) and was made possible by financial support from the Nederlandse Organisatie voor Wetenschappelijk Onderzoek (NWO).

CM0010102

(17) Burt, M. G.; Heine, V. *J. Phys. C: Solid State Phys.* **1978**, *11*, 961.

(18) Ebbinghaus, G.; Simon, A. *Chem. Phys.* **1970**, *43*, 117.

(19) Burroughes, J. H.; Bradley, D. D. C.; Brown, A. R.; Marks, R. N.; Mackey, K.; Friend, R. H.; Burn, P. L.; Holmes, A. B. *Nature* **1990**, *347*, 539.

(20) Park, I. D. *J. Appl. Phys.* **1994**, *75*, 1656. Sheats, J. R. *Science* **1997**, *277*, 191.

(21) Brown, A. R.; Pichler, K.; Greenham, N. C.; Bradley, D. D. C.; Friend, R. H. *Chem. Phys. Lett.* **1993**, *210*, 61. Sheats, J. R.; Roitman, D. B. *Synth. Met.* **1998**, *95*, 79.